Applied Physics Letters

Experimental implementation of tunable hybrid Tamm-microcavity modes

Cite as: Appl. Phys. Lett. **119**, 161107 (2021); https://doi.org/10.1063/5.0067179
Submitted: 14 August 2021 • Accepted: 01 October 2021 • Published Online: 20 October 2021

P. S. Pankin, V. S. Sutormin, V. A. Gunyakov, et al.

Applied Physics Letters ARTICLE scitation.org/journal/apl

Experimental implementation of tunable hybrid Tamm-microcavity modes

Cite as: Appl. Phys. Lett. **119**, 161107 (2021); doi: 10.1063/5.0067179
Submitted: 14 August 2021 · Accepted: 1 October 2021 ·
Published Online: 20 October 2021

P. S. Pankin,[1,2,a] V. S. Sutormin,[1,2] V. A. Gunyakov,[1] F. V. Zelenov,[3,4] I. A. Tambasov,[1] A. N. Masyugin,[3,4] M. N. Volochaev,[1,4] F. A. Baron,[1] K. P. Chen,[5] V. Ya. Zyryanov,[1] S. Ya. Vetrov,[1,2] and I. V. Timofeev[1,2]

AFFILIATIONS

[1]Kirensky Institute of Physics, Federal Research Center KSC SB RAS, 660036 Krasnoyarsk, Russia
[2]Siberian Federal University, Krasnoyarsk 660041, Russia
[3]AO NPP Radiosvyaz, 660021 Krasnoyarsk, Russia
[4]Reshetnev Siberian State University of Science and Technology, 660037 Krasnoyarsk, Russia
[5]National Yang Ming Chiao Tung University, 71150 Tainan, Taiwan

[a)]**Author to whom correspondence should be addressed:** pavel-s-pankin@iph.krasn.ru

ABSTRACT

Mode hybridization is a unique way to manipulate the mode inside a fixed cavity or at interface. For example, Tamm plasmon-polariton at solid interface can be spectrally shifted without tuning the interface. Experimental implementation of tunable hybrid Tamm-microcavity modes is reported. The hybrid modes are excited in a one-dimensional photonic crystal bounded with a gold layer by attaching a nematic liquid crystal microcavity. Coupling between Tamm plasmon-polariton and microcavity modes leads to repulsion of their dispersion curves controlled by the refractive index of a liquid crystal and the polarization of incident light. Effective tuning of hybrid modes through heating or applying an external electric field to the liquid crystal layer is demonstrated. The experimentally measured strength coupling value between Tamm and microcavity modes was 20.7 meV.

The Tamm plasmon-polariton (TPP) is an interface mode that occurs when light is trapped between two mirrors: a one-dimensional photonic crystal (PC) and a metal.[1–3] TPPs have been widely used in many applications, including topological phases,[4–8] absorbers for photovoltaics,[9–11] lasers,[12–14] single-photon emmitters[15] sensors and switches,[16–19] thermal emitters,[20–22] photoacoustic ultrasonic generators,[23] and nonlinear effect amplification.[2,24,25] TPP can couple to other types of modes in the system, forming hybrid modes, such as exciton,[26–30] surface plasmon-polariton,[31,32] or the microcavity (MC) mode.[33–35] Based on hybrid TPP-MC modes, organic solar cells,[36,37] white top-emitting organic light-emitting device,[38] the extraordinary field amplification,[39] metal layer absorption attenuation,[40] and hot-electron photodetector[41] were proposed.

The wide range of TPP applications makes the task of its efficient control relevant. The spectral position of the TPP can be adjusted in advance by changing the thickness of the first layer adjacent to the metal or by selecting the parameters of the PC and metal themselves.[1,42] However, more significant is the dynamic control of TPP and hybrid TPP modes, which is carried out after the fabrication of the sample. It can be realized by changing the incidence angle or polarization of the incident radiation,[1,32] mechanical scanning over the sample with variable first layer thickness[27,34] or mechanical changes in the thickness of the structure layers.[43] More dynamic control is possible by applying voltage to the first layer containing graphene[44] or quantum walls.[45,46] Heating the first layer made of liquid crystal (LC)[47] or including quantum wells[48] leads to a similar effect.

In this paper, we experimentally implemented the idea of dynamically controlling the spectral position of hybrid TPP-MC modes without changing the first layer at the interface. The idea is to affect TPP indirectly from outside, by means of coupled MC modes.[49] To demonstrate the effective control of hybrid modes, the microcavity layer was made of LC, whose refractive index was changed under the influence of an applied external electric field or heating.

The microcavity design supporting the existence of hybrid TPP-MC modes is shown in Fig. 1(a). The microcavity fabrication process includes following steps: (i) fabrication of PC and PC/Au mirrors. The mirrors of the microcavity are two identical one-dimensional PCs on a glass substrate consisting of 9 alternating layers of silicon dioxide (SiO_2) and silicon nitride (Si_3N_4) with thicknesses about 112 and 72 nm, respectively [Fig. 1(b)]. Alternating PC layers were grown by

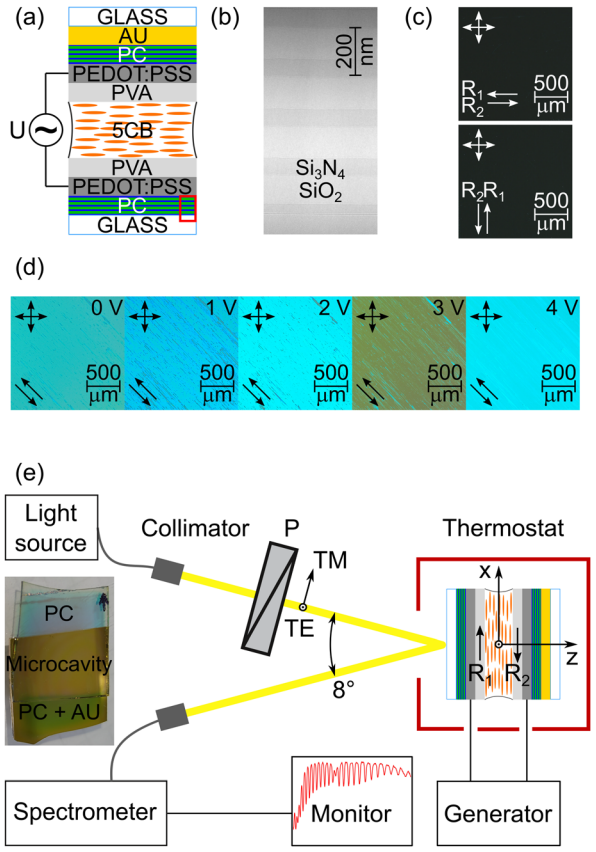

FIG. 1. (a) Schematic of the investigated structure. The area in the red rectangle corresponds to (b); (b) photograph of the PC obtained with an electron microscope; (c) photographs of the LC layer texture obtained with an optical microscope in crossed polarizers. The angle between the rubbing direction of the PVA layers ***R*** and the polarizer axis is 0° (top square) and 90° (bottom square); (d) change in the optical texture of the LC layer under the action of the applied electric field. The angle between the rubbing direction of the PVA layers ***R*** and the polarizer axis is 45°. (e) Schematic of the experiment to control the hybrid modes by the electric field and temperature change. The TM and TE vectors show the direction of the electric field vector for the respective polarizations. The inset shows a photograph of the microcavity.

the plasma enhanced chemical vapor deposition method. An opaque layer of gold (Au) about 200 nm thick was deposited between one of the PC and the substrate by magnetron sputtering; (ii) deposition of the conducting layers poly(3,4-ethylenedioxythiophene)-poly(styrenesulfonate) (PEDOT:PSS) (about 100 nm thick) on the PCs by spin-coating method; (iii) deposition of the alignment layers poly(vinyl alcohol) (PVA) (about 600 nm thick) by a spin-coating method. Unidirectional mechanical rubbing of PVA layers; (iv) creating a microcavity by gluing mirrors on UV-glue mixed with spherical spacers to control the gap thickness about 6.8 μm. Filling the gap with nematic LC 4-pentyl-4′-cyanobiphenyl (5CB) by exploiting of the capillary effect. Rubbed PVA layers are necessary to obtain the planar orientation of the LC director. Layers of the transparent conductive polymer PEDOT:PSS allow an external electric field perpendicular to the LC layer to be applied to the microcavity.

Photographs of the optical textures of the LC layer obtained in the crossed polarizer scheme are shown in Figs. 1(c) and 1(d). When the rubbing direction of the PVA ***R*** is parallel to the axis of one of the polarizers, the optical texture is a homogeneous dark region [Fig. 1(c)]. When the sample is rotated 45°, the maximum intensity of reflected light is observed. These optical textures indicate the realization of the planar orientation of the director. Applying an external AC voltage of 1 kHz to the LC layer leads to a change in the color of the optical texture, indicating an effective rearrangement of the LC structure [Fig. 1(d)]. A scheme for measuring the spectra of small-angle (4°) reflection of the microcavity, when linearly polarized light is incident on it, is shown in Fig. 1(e). Two independent ways of controlling the spectrum of the microcavity have been realized. The first approach used a 1 kHz alternating electrical voltage of varying magnitude applied to the microcavity using a function generator. The second approach involved the temperature variation of the sample using a thermostable cuvette, allowing it to be heated to temperatures above the LC-isotropic liquid phase transition, or cooled back to room temperature.

The reflection spectra of both mirrors of the microcavity are shown in Fig. 2(a). One of them shows a reflection band centered around 630 nm, corresponding to the photonic bandgap of the PC. The spectrum of the gold-coated PC mirror shows a resonance trough indicating TPP excitation at a wavelength of $\lambda_{TPP} = 608$ nm. The position of λ_{TPP} is determined by the different thickness of the first Si_3N_4 layer adjacent to the metal,[1] which in our case is about 42 nm [Fig. 1(b)]. The resonance dip corresponding to TPP almost reaches zero reflection, which corresponds to its critical coupling with incident light.[20] When the two mirrors are combined, an air-gap microcavity is formed, whose spectrum is shown in Fig. 2(b). Multiple resonances corresponding to MC modes can be seen, with a split resonance at wavelengths close to λ_{TPP}, indicating the formation of coupling between the TPP and MC modes. When the gap is filled with LC, there is an increase in the number of resonances [Figs. 2(c) and 2(d)] due to an increase in the optical thickness of the microcavity layer. At the same time, the reflection spectra become different for the TM-polarized (with components H_y, E_x, E_z) [Fig. 2(c)] or TE-polarized (with components E_y, H_x, H_z) [Fig. 2(d)] light waves. Because of the small angle of incidence of light ($E_z \ll E_x$), it can be assumed that in the case of TM-polarization, the electric field vector of the light wave is oriented along the direction of the LC director ***R***, while in the case of TE-polarization, it is orthogonal to the director. Because of the difference in the ordinary $n_e = 1.73$ and extraordinary $n_o = 1.52$ refractive indices of the LC, the number of resonances in the spectra for different polarizations is different; however, in both cases, a split resonance near λ_{TPP} is observed indicating the formation of hybrid TPP-MC modes.

The spectra of TE-polarized light do not change when a voltage is applied to the LC layer. This is due to the fact that the external electric field is directed along the z axis [Fig. 1(e)], which does not cause the molecules to rotate in the xy plane. Thus, for TE-polarized radiation, the refractive index of the LC layer is n_o regardless of the magnitude of the applied voltage. The TM-polarized spectrum undergoes a significant transformation [Fig. 2(e)] starting from the Frederiks threshold voltage $U_c = 0.74$ V. Under the action of an applied external electric field, the Frederiks transition occurs in the LC layer and the director tends to orient itself along the z axis.[50] The effective refractive index of the LC for the TM polarization n_e decreases,[51] which leads to

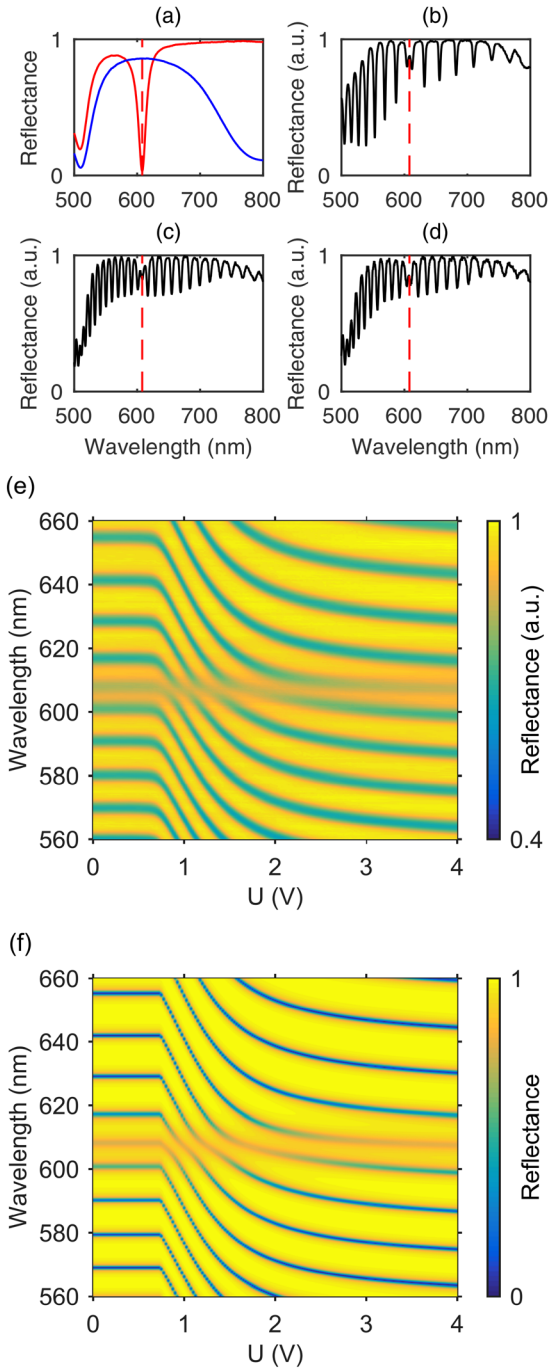

FIG. 2. (a) Reflectance of two PC mirrors of the microcavity measured at normal incidence for PC without (blue line) and with a gold layer (red line). The dotted red line shows the position of the resonance associated with the TPP excitation in the PC coated with the gold layer. (b)–(d) Reflectance of the microcavity taken at an incidence angle of 4°. (b) Air-gap microcavity, unpolarized incident light. Microcavity filled with LC, TM- (c) or TE- (d) polarized incident light. [(e) and (f)] Transformation of the reflectance shown in (c) when an external electric field is applied. Result of measurement (e) and numerical simulation (f). The spectra of the microcavity filled with LC were taken at $t = 21.8$°C.

a decrease in the optical thickness of the LC layer and a blue shift in the resonances of the MC modes.[52,53] Each MC mode passing through the blue shift through the wavelength $\lambda_{TPP} = 608$ nm experiences avoided crossing, indicating coupling with TPP and the formation of hybrid TPP-MC modes. The numerical calculation of the reflectance by the Berreman transfer matrix[54,55] method is in good agreement with the measured spectra [Fig. 2(f)]. To model the Frederiks transition, the LC free energy variation[56] method was used, which was described in detail for the investigated structure in Ref. 49. When the voltage amplitude is reduced back to 0 V, the resonances pass through the same positions in the reverse order, indicating that the microcavity is inherently more stable.

In contrast to the case when an electric field is applied to the LC layer, its heating leads to a transformation of the spectra in both TM-polarized [Fig. 3(a)] and TE-polarized incident waves [Fig. 3(b)]. An increase in the thermal motion of LC molecules leads to a decrease in the degree of ordering of the molecules in the rubbing direction of the PVA layer, resulting in a decrease in the extraordinary refractive index n_e and an increase in the ordinary refractive index n_o.[50] This leads to a

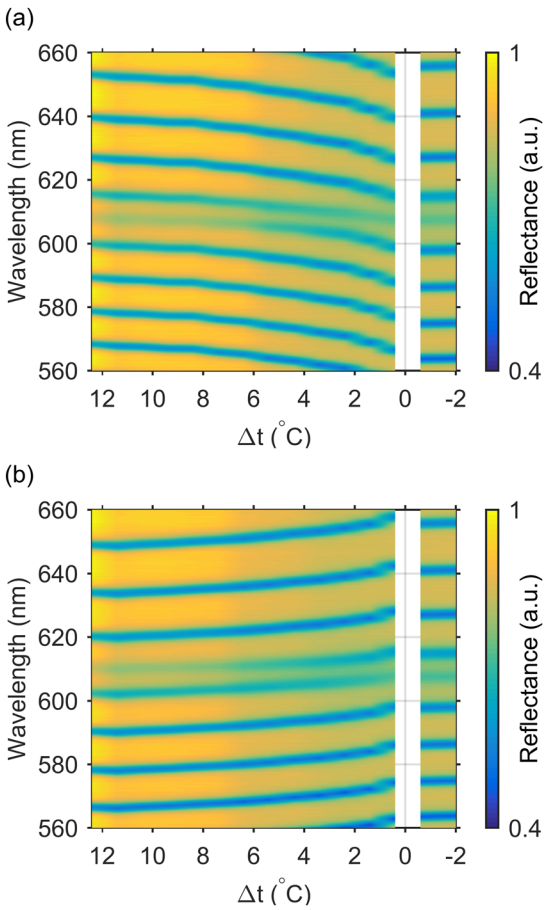

FIG. 3. Transformation of the measured microcavity reflection spectra, depending on the difference $\Delta t = t_0 - t$ between the temperature t of the LC layer and the phase transition temperature of LC – isotropic liquid $t_0 = 33.4$° C; (a) TM- or (b) TE-polarized light incident at angle 4°.

blue shift of MC mode resonances in the TM-polarized spectrum and a red shift for TE polarization,[57] respectively. As a result of the blue [Fig. 3(a)] or red [Fig. 3(b)] shift, the MC mode crossing the position $\lambda_{TPP} = 608$ nm experiences, as in the case of an applied electric field, avoided crossing, indicating coupling with TPP and formation of hybrid TPP-MC modes. When the temperature $t_0 = 33.4\,^{\circ}\mathrm{C}$ of the phase transition of the nematic-isotropic liquid is reached, the refractive indices jump[50] leading to the jump of MC[57] and hybrid TPP-MC modes.[49] Above the phase transition temperature, the spectra for TM- and TE-polarized light coincide. Reversibility of the microcavity, as in the case of electric control, is confirmed by passing the resonances through the same positions in the reverse order when cooling the sample back to room temperature.

To explain the behavior of resonances in the measured temperature spectra, it is convenient to consider the model of coupled oscillators[58] according to which the eigen circular frequencies ω of hybrid modes can be found by equating the determinant of the corresponding matrix to zero,

$$\begin{vmatrix} \omega - \omega_{TPP} & \Omega_{TPP-MC} \\ \Omega_{TPP-MC} & \omega - \omega_{MC} \end{vmatrix} = 0. \quad (1)$$

The eigenangular frequency $\omega_{TPP} = 10.3342\,\mu\mathrm{m}^{-1} = const$ of bare TPP was taken from the experimental spectrum of the Au-DBR mirror [Fig. 2(a)]. The eigenfrequency $\omega_{MC} = \omega_{MC}(t)$ of the bare MC mode as a function of temperature t was found analytically through solving the dispersion equation for MC modes obtained using the wave matching method, which was detailed for the PC with defect in the supplementary material.[59] The parameter Ω_{TPP-MC} characterizing the coupling strength between the modes was estimated from the experimental spectrum [Fig. 3(b)] using the value of the frequency splitting of the coupled modes $\Delta\omega = 2\Omega_{TPP-MC} \approx 0.105\,\mu\mathrm{m}^{-1}$ (which is equivalent to $\Delta\lambda \approx 6$ nm or $\Delta E \approx 20.7$ meV) at $\omega_{MC}(t) = \omega_{TPP}$.[60] Figure 4 compares the measured, numerical, and analytical spectra. The left panel contains the result of the numerical calculation by the Berreman method. The experimental spectrum is presented in the right panel. The analytical solution for bare MC modes is superimposed on the experimental spectrum as black dashed lines. The analytical solution for hybrid TPP-MC modes obtained in the coupled oscillator model according to Eq. (1) is also presented in the right panel of Fig. 4 as magenta dashed lines. This solution explains the avoided crossing behavior due to coupling between two modes. It can be seen that the spectral shift of the hybrid modes is directed from the TPP position and increases on approaching the TPP wavelength $\lambda_{TPP} = 608$ nm. The best agreement between the solution obtained in the coupled oscillator model and the experimental position of the resonances corresponding to the hybrid modes is observed near the point $\omega_{MC}(t) = \omega_{TPP}$. The insignificant difference far from this point can be explained by the fact that TPP is coupled with two adjacent MC modes at once, as it was described in Ref. 49. In this case, the model of three coupled oscillators[33] can be applied by analogy. It is worth noting that the presence of coupling between the modes is also indicated by the fact that the amplitudes of the split peak of the hybrid modes vary with the external control parameter. The parameter is the amplitude of the applied external electric field [Fig. 2(f)] or temperature (Fig. 3).

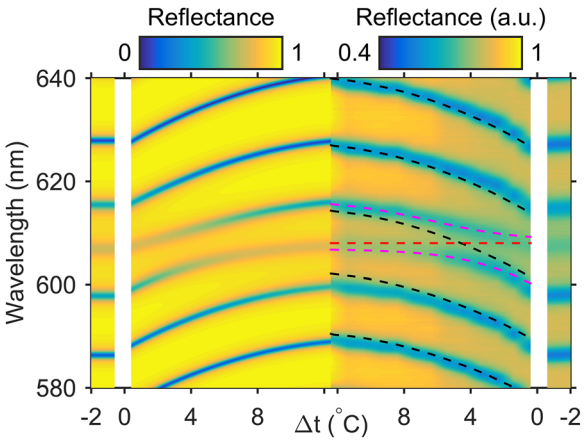

FIG. 4. Calculated (left panel) and measured (right panel) temperature reflectance spectra for TM-polarized incident light at 4°. The measured spectrum corresponds to Fig. 3(a) and is taken at an enlarged scale. The position of the bare TPP taken from Fig. 2(a) (red dashed line); the position of the MC modes obtained from the solution of the dispersion equation (black dashed line); the solution of Eq. (1) for the coupled oscillator model (magenta dashed line).

In summary, the electrically and temperature-controlled hybrid TPP-MC modes have been experimentally implemented for the first time. The presented approach made it possible to manipulate the TPP wavelength by affecting the coupled modes externally without changing the structure in which TPP is localized. Based on the advanced LC-cell technology platform, the device opens up broad possibilities for introducing TPP into modern photonics applications.

See the supplementary material for additional information on sample fabrication, experimental setup, calculation parameters, estimation of electric heating effect value, and additional figures.

The authors are grateful to M. N. Krakhalev for helpful discussions. Electrical control of hybrid modes was funded by Russian Foundation for Basic Research, Government of Krasnoyarsk Territory, Krasnoyarsk Region Science and Technology Support Fund to the research, Project No. 19-42-240004. Temperature control of hybrid modes was funded by Russian Foundation for Basic Research, Project No. 19-52-52006 and No. MOST 108-2923-E-009-003-MY3, Taiwan. P. S. Pankin is grateful for the support of the President of the Russian Federation under Grant No. MK-4012.2021.1.2. This study was supported by the Krasnoyarsk Regional Center of Research Equipment of Federal Research Center KSC SB RAS.

DATA AVAILABILITY

The data that support the findings of this study are available within the article and its supplementary material.

REFERENCES

[1]M. Kaliteevski, I. Iorsh, S. Brand, R. A. Abram, J. M. Chamberlain, A. V. Kavokin, and I. A. Shelykh, "Tamm plasmon-polaritons: Possible electromagnetic states at the interface of a metal and a dielectric Bragg mirror," Phys. Rev. B **76**, 165415 (2007).

[2]A. P. Vinogradov, A. V. Dorofeenko, S. G. Erokhin, M. Inoue, A. A. Lisyansky, A. M. Merzlikin, and A. B. Granovsky, "Surface state peculiarities in one-dimensional photonic crystal interfaces," Phys. Rev. B **74**, 045128 (2006).

[3]M. E. Sasin, R. P. Seisyan, M. A. Kalitteevski, S. Brand, R. A. Abram, J. M. Chamberlain, A. Y. Egorov, A. P. Vasil'ev, V. S. Mikhrin, and A. V. Kavokin, "Tamm plasmon polaritons: Slow and spatially compact light," Appl. Phys. Lett. **92**, 251112 (2008).
[4]Q. Wang, M. Xiao, H. Liu, S. Zhu, and C. T. Chan, "Measurement of the Zak phase of photonic bands through the interface states of a metasurface/photonic crystal," Phys. Rev. B **93**, 041415 (2016).
[5]Q. Wang, M. Xiao, H. Liu, S. Zhu, and C. T. Chan, "Optical interface states protected by synthetic weyl points," Phys. Rev. X **7**, 031032 (2017).
[6]Y. Tsurimaki, J. K. Tong, V. N. Boriskin, A. Semenov, M. I. Ayzatsky, Y. P. Machekhin, G. Chen, and S. V. Boriskina, "Topological engineering of interfacial optical Tamm states for highly sensitive near-singular-phase optical detection," ACS Photonics **5**, 929–938 (2018).
[7]H. Lu, Y. Li, Z. Yue, D. Mao, and J. Zhao, "Topological insulator based Tamm plasmon polaritons," APL Photonics **4**, 040801 (2019).
[8]C. Schmidt, A. Palatnik, M. Sudzius, S. Meister, and K. Leo, "Coupled topological interface states," Phys. Rev. B **103**, 085412 (2021).
[9]X.-L. Zhang, J.-F. Song, X.-B. Li, J. Feng, and H.-B. Sun, "Optical Tamm states enhanced broad-band absorption of organic solar cells," Appl. Phys. Lett. **101**, 243901 (2012).
[10]A. M. Vyunishev, R. G. Bikbaev, S. E. Svyakhovskiy, I. V. Timofeev, P. S. Pankin, S. A. Evlashin, S. Y. Vetrov, S. A. Myslivets, and V. G. Arkhipkin, "Broadband Tamm plasmon polariton," J. Opt. Soc. Am. B **36**, 2299 (2019).
[11]R. G. Bikbaev, S. Y. Vetrov, I. V. Timofeev, and V. F. Shabanov, "Photosensitivity and reflectivity of the active layer in a Tamm-plasmon-polariton-based organic solar cell," Appl. Opt. **60**, 3338 (2021).
[12]C. Symonds, A. Lemaître, P. Senellart, M. H. Jomaa, S. Aberra Guebrou, E. Homeyer, G. Brucoli, and J. Bellessa, "Lasing in a hybrid GaAs/silver Tamm structure," Appl. Phys. Lett. **100**, 121122 (2012).
[13]A. R. Gubaydullin, C. Symonds, J. Bellessa, K. A. Ivanov, E. D. Kolykhalova, M. E. Sasin, A. Lemaître, P. Senellart, G. Pozina, and M. A. Kaliteevski, "Enhancement of spontaneous emission in Tamm plasmon structures," Sci. Rep. **7**, 9014 (2017).
[14]S. Meister, R. Brückner, M. Sudzius, H. Fröb, and K. Leo, "Optically pumped lasing of an electrically active hybrid OLED-microcavity," Appl. Phys. Lett. **112**, 113301 (2018).
[15]O. Gazzano, S. Michaelis de Vasconcellos, K. Gauthron, C. Symonds, P. Voisin, J. Bellessa, A. Lemaître, and P. Senellart, "Single photon source using confined Tamm plasmon modes," Appl. Phys. Lett. **100**, 232111 (2012).
[16]B. I. Afinogenov, A. A. Popkova, V. O. Bessonov, and A. A. Fedyanin, "Measurements of the femtosecond relaxation dynamics of Tamm plasmon-polaritons," Appl. Phys. Lett. **109**, 171107 (2016).
[17]S. Kumar and R. Das, "Refractive index sensing using a light trapping cavity: A theoretical study," J. Appl. Phys. **123**, 233103 (2018).
[18]B. I. Afinogenov, V. O. Bessonov, I. V. Soboleva, and A. A. Fedyanin, "Ultrafast all-optical light control with Tamm plasmons in photonic nanostructures," ACS Photonics **6**, 844–850 (2019).
[19]E. Harbord, B. Cemlyn, M. Parker, E. Clarke, K. Kennedy, I. Henning, M. Adams, and R. Oulton, "Confined Tamm optical states coupled to quantum dots in a photoconductive detector," Appl. Phys. Lett. **115**, 171101 (2019).
[20]Z.-Y. Yang, S. Ishii, T. Yokoyama, T. D. Dao, M.-G. Sun, P. S. Pankin, I. V. Timofeev, T. Nagao, and K.-P. Chen, "Narrowband wavelength selective thermal emitters by confined Tamm plasmon polaritons," ACS Photonics **4**, 2212–2219 (2017).
[21]Z. Wang, J. K. Clark, Y.-L. Ho, B. Vilquin, H. Daiguji, and J.-J. Delaunay, "Narrowband thermal emission from Tamm plasmons of a modified distributed Bragg reflector," Appl. Phys. Lett. **113**, 161104 (2018).
[22]Z. Yang, S. Ishii, A. T. Doan, S. L. Shinde, T. D. Dao, Y. Lo, K. Chen, and T. Nagao, "Narrow-band thermal emitter with titanium nitride thin film demonstrating high temperature stability," Adv. Opt. Mater. **8**, 1900982 (2020).
[23]E. I. Girshova, A. P. Mikitchuk, A. V. Belonovski, K. M. Morozov, K. A. Ivanov, G. Pozina, K. V. Kozadaev, A. Y. Egorov, and M. A. Kaliteevski, "Proposal for a photoacoustic ultrasonic generator based on Tamm plasmon structures," Opt. Express **28**, 26161 (2020).
[24]B. I. Afinogenov, V. O. Bessonov, and A. A. Fedyanin, "Second-harmonic generation enhancement in the presence of Tamm plasmon-polaritons," Opt. Lett. **39**, 6895 (2014).
[25]B. I. Afinogenov, A. A. Popkova, V. O. Bessonov, B. Lukyanchuk, and A. A. Fedyanin, "Phase matching with Tamm plasmons for enhanced second- and third-harmonic generation," Phys. Rev. B **97**, 115438 (2018).
[26]C. Symonds, A. Lemaître, E. Homeyer, J. C. Plenet, and J. Bellessa, "Emission of Tamm plasmon/exciton polaritons," Appl. Phys. Lett. **95**, 151114 (2009).
[27]S. S.-U. Rahman, T. Klein, S. Klembt, J. Gutowski, D. Hommel, and K. Sebald, "Observation of a hybrid state of Tamm plasmons and microcavity exciton polaritons," Sci. Rep. **6**, 34392 (2016).
[28]T. Hu, Y. Wang, L. Wu, L. Zhang, Y. Shan, J. Lu, J. Wang, S. Luo, Z. Zhang, L. Liao, S. Wu, X. Shen, and Z. Chen, "Strong coupling between Tamm plasmon polariton and two dimensional semiconductor excitons," Appl. Phys. Lett. **110**, 051101 (2017).
[29]Z. Wang, R. Gogna, and H. Deng, "What is the best planar cavity for maximizing coherent exciton-photon coupling," Appl. Phys. Lett. **111**, 061102 (2017).
[30]K. M. Morozov, P. Pander, L. G. Franca, A. V. Belonovski, E. I. Girshova, K. A. Ivanov, D. A. Livshits, N. V. Selenin, G. Pozina, A. P. Monkman, and M. A. Kaliteevski, "Opposite sign of polarization splitting in ultrastrongly coupled organic Tamm plasmon structures," J. Phys. Chem. C **125**, 8376–8381 (2021).
[31]A. V. Baryshev, K. Kawasaki, P. B. Lim, and M. Inoue, "Interplay of surface resonances in one-dimensional plasmonic magnetophotonic crystal slabs," Phys. Rev. B **85**, 205130 (2012).
[32]B. I. Afinogenov, V. O. Bessonov, A. A. Nikulin, and A. A. Fedyanin, "Observation of hybrid state of Tamm and surface plasmon-polaritons in one-dimensional photonic crystals," Appl. Phys. Lett. **103**, 061112 (2013).
[33]M. Kaliteevski, S. Brand, R. A. Abram, I. Iorsh, A. V. Kavokin, and I. A. Shelykh, "Hybrid states of Tamm plasmons and exciton polaritons," Appl. Phys. Lett. **95**, 251108 (2009).
[34]R. Brückner, M. Sudzius, S. I. Hintschich, H. Fröb, V. G. Lyssenko, and K. Leo, "Hybrid optical Tamm states in a planar dielectric microcavity," Phys. Rev. B **83**, 033405 (2011).
[35]R. Brückner, M. Sudzius, S. I. Hintschich, H. Fröb, V. G. Lyssenko, M. A. Kaliteevski, I. Iorsh, R. A. Abram, A. V. Kavokin, and K. Leo, "Parabolic polarization splitting of Tamm states in a metal-organic microcavity," Appl. Phys. Lett. **100**, 062101 (2012).
[36]X.-L. Zhang, J.-F. Song, J. Feng, and H.-B. Sun, "Spectral engineering by flexible tunings of optical Tamm states and Fabry–Perot cavity resonance," Opt. Lett. **38**, 4382 (2013).
[37]X.-L. Zhang, J.-F. Song, X.-B. Li, J. Feng, and H.-B. Sun, "Light trapping schemes in organic solar cells: A comparison between optical Tamm states and Fabry–Pérot cavity modes," Organic Electron. **14**, 1577–1585 (2013).
[38]X.-L. Zhang, J. Feng, X.-C. Han, Y.-F. Liu, Q.-D. Chen, J.-F. Song, and H.-B. Sun, "Hybrid Tamm plasmon-polariton/microcavity modes for white top-emitting organic light-emitting devices," Optica **2**, 579 (2015).
[39]Y.-t. Fang, L.-x. Yang, W. Kong, and N. Zhu, "Tunable coupled states of a pair of Tamm plasmon polaritons and a microcavity mode," J. Opt. **15**, 125703 (2013).
[40]M. A. Kaliteevski, A. A. Lazarenko, N. D. Il'inskaya, Y. M. Zadiranov, M. E. Sasin, D. Zaitsev, V. A. Mazlin, P. N. Brunkov, S. I. Pavlov, and A. Y. Egorov, "Experimental demonstration of reduced light absorption by intracavity metallic layers in Tamm plasmon-based microcavity," Plasmonics **10**, 281–284 (2015).
[41]R. Li, C. Zhang, and X. Li, "Schottky hot-electron photodetector by cavity-enhanced optical Tamm resonance," Appl. Phys. Lett. **110**, 013902 (2017).
[42]C. Y. Chang, Y. H. Chen, Y. L. Tsai, H. C. Kuo, and K. P. Chen, "Tunability and optimization of coupling efficiency in Tamm plasmon modes," IEEE J. Sel. Top. Quantum Electron. **21**, 262–267 (2015).
[43]C. Grossmann, G. Christmann, J. J. Baumberg, I. Farrer, H. Beere, and D. A. Ritchie, "Strong coupling at room temperature in ultracompact flexible metallic microcavities," Appl. Phys. Lett. **102**, 011118 (2013).
[44]L. Li, H. Zhao, and J. Zhang, "Electrically tuning reflection of graphene-based Tamm plasmon polariton structures at 1550 nm," Appl. Phys. Lett. **111**, 083504 (2017).
[45]C. Grossmann, C. Coulson, G. Christmann, I. Farrer, H. E. Beere, D. A. Ritchie, and J. J. Baumberg, "Tuneable polaritonics at room temperature with strongly coupled Tamm plasmon polaritons in metal/air-gap microcavities," Appl. Phys. Lett. **98**, 231105 (2011).

[46]J. Gessler, V. Baumann, M. Emmerling, M. Amthor, K. Winkler, S. Höfling, C. Schneider, and M. Kamp, "Electro optical tuning of Tamm-plasmon exciton-polaritons," Appl. Phys. Lett. **105**, 181107 (2014).
[47]H.-C. Cheng, C.-Y. Kuo, Y.-J. Hung, K.-P. Chen, and S.-C. Jeng, "Liquid-crystal active tamm-plasmon devices," Phys. Rev. Appl. **9**, 64034 (2018).
[48]K. Sebald, S. S. Rahman, M. Cornelius, J. Gutowski, T. Klein, S. Klembt, C. Kruse, and D. Hommel, "Tailoring the optical properties of wide-bandgap based microcavities via metal films," Appl. Phys. Lett. **107**, 062101 (2015).
[49]P. S. Pankin, S. Y. Vetrov, and I. V. Timofeev, "Tunable hybrid Tamm-microcavity states," J. Opt. Soc. Am. B **34**, 2633–2639 (2017).
[50]L. M. Blinov, *Structure and Properties of Liquid Crystals*, Topics in Applied Physics (Springer, 2010), p. 458.
[51]M. Born and E. Wolf, *Principles of Optics: Electromagnetic Theory of Propagation, Interference and Diffraction of Light* (Cambridge University Press, 1999).
[52]S. Y. Vetrov and A. V. Shabanov, "Localized electromagnetic modes and the transmission spectrum of a one-dimensional photonic crystal with lattice defects," J. Exp. Theor. Phys. **93**, 977–984 (2001).
[53]V. G. Arkhipkin, V. A. Gunyakov, S. A. Myslivets, V. Y. Zyryanov, V. F. Shabanov, and W. Lee, "Electro- and magneto-optical switching of defect modes in one-dimensional photonic crystals," J. Exp. Theor. Phys. **112**, 577–587 (2011).
[54]D. W. Berreman, "Optics in stratified and anisotropic media: 4 × 4-matrix formulation," J. Opt. Soc. Am. **62**, 502–510 (1972).
[55]R. M. A. Azzam and N. M. Bashara, *Ellipsometry and Polarized Light* (North-Holland Pub. Co., 1977).
[56]H. J. Deuling, "Deformation of nematic liquid crystals in an electric field," Mol. Cryst. Liq. Cryst. **19**, 123–131 (1972).
[57]V. G. Arkhipkin, V. A. Gunyakov, S. A. Myslivets, V. P. Gerasimov, V. Y. Zyryanov, S. Y. Vetrov, and V. F. Shabanov, "One-dimensional photonic crystals with a planar oriented nematic layer: Temperature and angular dependence of the spectra of defect modes," J. Exp. Theor. Phys. **106**, 388–398 (2008).
[58]H. A. Haus, *Waves and Fields in Optoelectronics*, Prentice-Hall Series in Solid State Physical Electronics (Prentice Hall, Incorporated, Upper Saddle River, NJ, 1983), p. 402.
[59]P. S. Pankin, B.-R. Wu, J.-H. Yang, K.-P. Chen, I. V. Timofeev, and A. F. Sadreev, "One-dimensional photonic bound states in the continuum," Commun. Phys. **3**, 91 (2020).
[60]P. Das, S. Mukherjee, S. Jana, S. K. Ray, and B. N. Shivakiran Bhaktha, "Resonant and non-resonant coupling of one-dimensional microcavity mode and optical Tamm state," J. Opt. **22**, 065002 (2020).